Proceedings of ASME Turbo Expo 2015: Turbine Technical Conference and Exposition
GT2015
June 15 – 19, 2015, Montréal, Canada

GT2015-43382

NUMERICAL INVESTIGATION OF THE FLOW FIELD AND MIXING IN A SWIRL-STABILIZED BURNER WITH A NON-SWIRLING AXIAL JET

Tom Tanneberger*, Thoralf G. Reichel, Oliver Krüger,
Steffen Terhaar, Christian Oliver Paschereit
Chair of Fluid Dynamics
– Hermann-Föttinger-Institut –
Technische Universität Berlin
Müller-Breslau-Str. 8, 10623 Berlin, Germany

ABSTRACT

In the present study numerical results of simulations, using RANS and LES, of the non-reacting flow in a swirl-stabilized burner are presented. The burner was developed for lean premixed combustion with high fuel flexibility at low emissions. An important challenge for a fuel-flexible, low emission combustor is the prevention of flashback for fuels of high reactivity, such as hydrogen, without compromising on lean blow out safety and mixing quality. Flashback safety can be increased by a sufficiently high and uniform axial velocity at the end of the mixing tube. In the investigated combustor the velocity deficit in the center of the mixing tube, which results from the swirl, is prevented by a non-swirling axial jet. In a parametric study the effect of different amounts of axial injection on the flow field is investigated. The results are validated with experimental data, gained from PIV measurements in a vertical water tunnel. It is shown that the mean flow field can be well captured by steady-state RANS simulations using a realizable k-ε turbulence model. The most suitable geometry is identified and, subsequently, transient LES simulations are conducted. The dynamic flow field characteristics are investigated. It was found that in spite of the high swirl, the flow field is quite stable and no dominating frequency is detected. The flow field of the swirling flow in the combustion chamber can be captured well using LES. Furthermore, the mixing quality is compared to the experiments, which are performed in a water tunnel. In contrast to the RANS simulation, the LES can qualitatively capture the spatial unmixedness observed from experimental data. All simulations were conducted using water as fluid.

*Address all correspondence to this author, Tom.Tanneberger@tu-berlin.de

NOMENCLATURE

ε	turbulent dissipation rate
κ	von Kármán constant
ν	kinematic viscosity
ν_t	eddy viscosity
ρ	density
τ_{ij}	stress tensor
χ	ratio of non-swirled volume flow to total volume flow
C	concentration of the fuel agent
C^*	normalized, time-averaged fuel distribution
Co	Courant number
C_s	Smagorinsky constant
D	mixing tube diameter
D_{or}	orifice diameter
d	distance to the closest wall
E	energy spectrum function
f	frequency
I	light intensity
J	momentum ratio
k	turbulent kinetic energy
r	radial coordinate
Ma	Mach number
p	pressure
Re	Reynolds number
St	Strouhal number
S_{ij}	stress tensor of molecular viscosity
Tu	turbulence intensity
T_{ij}	subgrid-scale stress tensor
U	Danckwerts unmixedness parameter
u'	fluctuation of axial velocity
u_i	velocity components ($i = x, y, z$)
u_0	bulk velocity at the end of the mixing tube
u_{rms}	mean fluctuation of axial velocity

u_ϕ	mean tangential velocity
V	cell volume
$\dot{V}$	volume flow
x, y, z	coordinates
LES	Large Eddy Simulation
RANS	Reynolds Averaged Navier-Stokes Equations
RMS	Root Mean Square
PIV	Particle Image Velocimetry
PLIF	Planar Laser-Induced Fluorescence

INTRODUCTION

The aim for climate sensitive politics today is to reduce CO_2 and NO_x emissions in the processes of power generation. To fulfill these targets the conventional technologies need to reduce their emissions. Additionally, there has to be a steep growth of renewable energies. The latter leads to high fluctuations in the energy supply, which have to be regulated by highly flexible power plants. In the scope of the CleanGT project, which is founded by the EU's main climate innovation initiative Climate-KIC, a gas turbine technology is developed that combines low emissions with a high operational and fuel flexibility. Within this framework a low emission burner with a large range of applicable fuels was developed.

In modern gas turbines lean premixed combustion is preferred to reduce the NO_x emissions because it provides a low flame temperature and high mixing quality. An alternative concept is the RQL (Rich-Burn, Quick-Quench, Lean-Burn) combustion [1]. In order to stabilize a premixed flame, a local zone of low flow velocities, e.g. a shear layer, is needed. One concept to provide a stable shear layer for premixed combustion is to establish a swirl induced recirculation zone inside the combustion chamber [2]. The sudden expansion at the end of the mixing tube leads to vortex breakdown, which stabilizes the flame due to lowered velocities in the shear layer and by continuously feeding the flame with heat and combustion products. Since there is no bluff body, e.g. a center body, in the presented burner, one has to ensure that the recirculation zone does not propagate into the mixing tube, which would increase the risk of flashback. Especially in the sense of high fuel flexibility, the burner has to be designed flashback safe even for high reactivity fuels, e.g. hydrogen. Different flashback mechanisms are possible and have been identified in the literature. The current study only focusses on flashback on the centerline. Further mechanisms like flashback in the boundary layer on the combustor walls or high level fluctuations of the turbulent flame speed that overshoot the mean bulk velocity are not addressed by the following measure and not discussed in the current paper. The idea is to make the flow field less prone to combustion induced vortex breakdown (CIVB) by avoiding a velocity deficit at the centerline. In previous investigations of the burner at a combustion test rig, it was found that CIVB is by far the most common type of flashback in this combustor in the absence of axial injection [3].

A promising technique to avoid the velocity deficit on the central axis was reported by Burmberger and Sattelmayer [3, 4], who stated to influence the vortex breakdown position by using a non-swirling axial jet. Further measures are the reduction of the mixing tube length or the swirl number [4]. Reichel et al [6] investigated the latter two techniques for the present burner and revealed that they both impaired the spatial and temporal mixing quality. On the other hand, using the axial injection into the swirling flow, Reichel et al. [3] reached an improvement of the temporal mixing quality, while the spatial unmixedness was only marginally increased. In the sense of emission reduction, the mixing quality plays an important role because high unmixedness leads to locally higher equivalence ratios and, thus, to higher NO_x emissions.

A second phenomenon regarding swirl-stabilized burners is the occurrence of large-scale flow instability in the combustion chamber. Lucca-Negro and O'Doherty [7] provide a broad overview to the topic of vortex breakdown and related flow instabilities. The dynamics of lean-premixed swirl-stabilized combustion in general were discussed by Huang and Yang [8]. Hydrodynamic instabilities, e.g. the precessing vortex core, were observed in the actual and similar burners without axial injection ([7, 8]). Various investigations, especially for the current burner, reveal that the flow field in the presence of a non-swirling axial jet is less prone to exhibit self-exited flow oscillations ([7, 9–11]).

Since experimental investigations are costly and time consuming, while computational performance increases from year to year, numerical simulations get more and more in the focus of research and development in the gas turbine community. Of course, these methods have to be validated of being capable of delivering the correct physical behavior especially for complex flows like that in a swirl-stabilized burner. Numerical simulations have been successfully used by many authors to describe swirling flows, e.g. [14–16]. For such flows LES is a preferable technique as it provides more accurate and reliable results than RANS. Nevertheless RANS is much faster and less expensive. Thus, it is commonly used for gaining fast results in parameter studies and is also applied within this work. Due to the fact that LES computes the large-scale motion of the turbulence that contains most of the turbulent kinetic energy directly, LES is better suited for the investigation of dynamic flow structures.

In the present work a numerical parameter study is conducted to find the optimal amount of axial injection of a non-swirled jet for a stable stagnation point downstream of the burner exit. Therefore the axial flow ratio χ and the amount of fuel injection were varied. Taking the optimized geometry, further investigations of mixing and flow instabilities are conducted. Regarding the mixing process, the question is whether RANS and/or LES are capable of reproducing experimental data and if the burner provides sufficient mixing in spite of the axial jet. Since the LES simulation delivers a transient and three dimensional flow and mixing field, the provided information should be more valuable than in previous investigations ([3], [6]), that where based on two dimensional PIV. Regarding the flow dynamics the investigation focusses on the suppression of previously observed instabilities ([8, 16]) in the burner.

In order to compare the simulations to experimental data from a water tunnel facility, the simulations are conducted isothermally with water as fluid for the main flow as well as for the fuel injection. The Reynolds number and the fuel-air momentum ratio are kept equivalent to gas-fired tests [3].

METHODS

Governing Equations

Due to the fact that the simulation is conducted with water and the velocities are below $Ma = 0.3$, the motion of the fluid can be described with the incompressible conservation of mass and momentum, which are stated in the Navier-Stokes equations and read as follows:

Continuity:
$$\frac{\partial u_i}{\partial x_i} = 0 \tag{1}$$

Momentum Conservation:
$$\frac{\partial u_i}{\partial t} + \frac{\partial u_i u_j}{\partial x_j} = -\frac{1}{\rho}\frac{\partial p}{\partial x_i} + \frac{\partial}{\partial x_j}\tau_{ij} \tag{2}$$

Stress tensor:
$$\frac{\partial}{\partial x_i}\tau_{ij} = \nu\frac{\partial^2 u_i}{\partial x_j \partial x_i} \tag{3}$$

In these equations u_i denotes a velocity component, p the pressure, ρ the density and τ_{ij} the stress tensor. In this paper the turbulence is modeled in two different ways: *Reynolds Averaged Navier-Stokes equations* (RANS) and *Large Eddy Simulations* (LES).

RANS

Within the RANS approach the whole flow field is Reynolds decomposed in a mean and a fluctuating component $u = \bar{u} + u'$. Applying this decomposition to the conservation equations followed by time averaging leads to the Reynolds Averaged Navier-Stokes equations for incompressible steady-state flows:

$$\frac{\partial \bar{u}_i}{\partial x_i} = 0 \tag{4}$$

$$\frac{\partial \bar{u}_i \bar{u}_j}{\partial x_j} = -\frac{1}{\rho}\frac{\partial p}{\partial x_i} + \frac{\partial}{\partial x_j}\left(-\overline{u_i' u_j'}\right) + \frac{\partial}{\partial x_j}\left[\nu\left(\frac{\partial \bar{u}_i}{\partial x_j} + \frac{\partial \bar{u}_i}{\partial x_j} - \frac{2}{3}\delta_{ij}\frac{\partial \bar{u}_l}{\partial x_l}\right)\right]. \tag{5}$$

This system of equations is under-determined due to the Reynolds stresses $\overline{u_i' u_j'}$. They have to be modeled. In the present simulations this is done by using a realizable k-ε turbulence model proposed by Shih [17]. As pressure-velocity coupling, the RANS simulations use a coupled algorithm, which solves the momentum and pressure-based continuity equations simultaneously.

LES

In an LES the large scale turbulent fluctuations are computed, while the small scales are modeled. Therefore, the time dependent Navier-Stokes equations of the flow field are "low pass" filtered. The following equations for continuity and momentum are obtained:

$$\frac{\partial}{\partial x_i}(\tilde{u}_i) = 0 \tag{6}$$

$$\frac{\partial \tilde{u}_i}{\partial t} + \frac{\partial \tilde{u}_i \tilde{u}_j}{\partial x_j} = -\frac{1}{\rho}\frac{\partial \tilde{p}}{\partial x_i} + \frac{\partial S_{ij}}{\partial x_j} - \frac{\partial T_{ij}}{\partial x_j}. \tag{7}$$

They include the stress tensor due to molecular viscosity

$$S_{ij} = \left[\nu\left(\frac{\partial \tilde{u}_i}{\partial x_j} + \frac{\partial \tilde{u}_j}{\partial x_i}\right)\right] - \frac{2}{3}\nu\frac{\partial \widetilde{u_l}}{\partial x_l}\delta_{ij} \tag{8}$$

and the subgrid-scale stress tensor

$$T_{ij} = \widetilde{u_i u_j} - \tilde{u}_i \tilde{u}_j, \tag{9}$$

which cannot be expressed as filtered equations and thus are unknown subgrid terms that require modeling. The subgrid stresses are calculated using the Boussinesq hypothesis [18]:

$$T_{ij} - \frac{1}{3}T_{kk}\delta_{ij} = -2\nu_t \tilde{S}_{ij} \tag{10}$$

$$\tilde{S}_{ij} \equiv \frac{1}{2}\left(\frac{\partial u_i}{\partial x_j} + \frac{\partial u_j}{\partial x_i}\right). \tag{11}$$

For modeling the eddy-viscosity ν_t the Smagorinsky-Lilly model [19] was chosen.

$$\nu_t = L_s^2\left|\tilde{S}\right|. \tag{12}$$

Here, L_s represents the mixing length for subgrid scales, calculated by $L_s = \min\left(\kappa d, C_s V^{\frac{1}{3}}\right)$, where κ is the von Kármán constant, d the distance to the closest wall, V the cell volume and C_s the Smagorinsky constant, which was set to $C_s = 0.1683$, according to validated simulations of a similar swirl stabilized burner [20].

For the pressure-velocity coupling the *Pressure-Implicit with Splitting of Operators* (PISO) scheme is used.

SETUP

The investigated burner

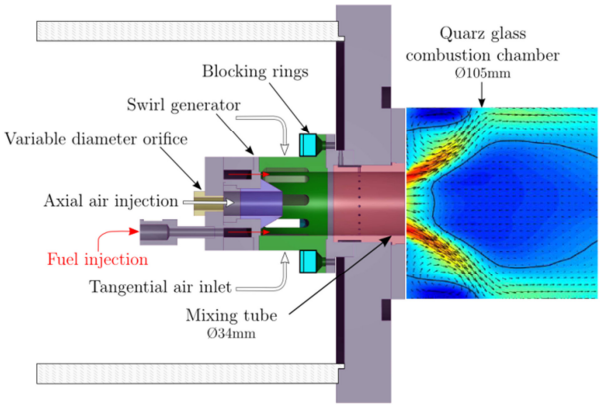

FIGURE 1: SCHEMATIC OF THE SWIRL-STABILIZED BURNER

The burner is shown in Figure 1 and consists of two oxidizer inlets, a radial swirler and an orifice on the central axis, which are fed by a shared plenum. The unit of swirler and mixing tube is denoted in the following as burner, whereas the burner with the combustion chamber is referred to as combustor. The ratio of the axial non-swirling flow to the overall inlet flow is defined as $\chi = \dot{V}_{ax}/(\dot{V}_{ax} + \dot{V}_{sw})$ and is only determined by the pressure losses of both components. χ and thus the intensity of the axial jet is varied by the diameter of the orifice D_{or}. The axial jet, added through a hollow cone (purple), and the swirled flow, added through the swirl generator (green), enter a mixing tube of 60 mm length and $D = 34$ mm diameter. At the end of the mixing tube, the mixture flows over a backward-facing step with a diameter ratio of 3.1 into the combustion chamber. The combustion chamber in the experiment has a length of 17.6 D, which was reduced in the simulations to 8.8 D, in order to reduce the number of grid cells in the far upstream flow region. The fuel is injected into the mixing tube through 16 injection holes of 1.6 mm diameter each. They are located on an annular ring between the cone and the swirler inlets. For detailed information of the burner see Ref. [6].

Numerical setup

The numerical simulations of the present paper were conducted using the commercial Ansys Fluent 14.5 CFD solver. Steady-state RANS simulations are examined for a parametric study of the geometry. One configuration is investigated with LES to gain time resolved velocity and mixing data.

The simulations are performed on two domains, a full one, which consists of the whole combustor including the plenum and the swirler, and a reduced one which only consists of the mixing tube and the combustion chamber as depicted in yellow in Figure 2. The inlet boundary conditions of the reduced domain are mapped from the results of the RANS simulation of the full domain. Several authors reported about using inlet profiles from previous simulations or measurements instead of simulating the whole combustor including the swirl generator [9], [21–23]. The LES simulations are only conducted on the cropped domain, which reduces the computational effort at least about 35 %. Dependent on the burner geometry, this gain can be even higher for more complex swirl generators.

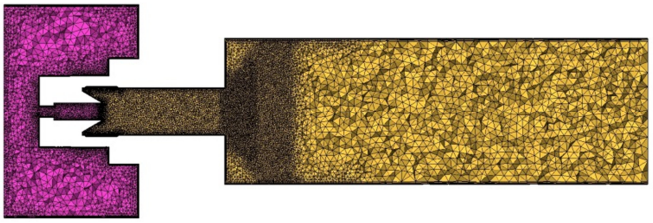

FIGURE 2: SIMULATION DOMAIN OF THE FULL (MAGENTA) AND THE REDUCED (YELLOW) MESH

TABLE 1: NUMERICAL SETUPS

Condition	Case 1	Case 2	Case 3
Name	RANS full	RANS cropped	LES cropped
Simulation type	RANS	RANS	LES
Fluid	Water	Water	Water
Turbulence model / Subgrid-scale model	Realizable k-ε	Realizable k-ε	Smagorinsky-Lilly
Inlet BC	Mass flow inlet	Velocity inlet	Velocity inlet
Outlet BC	Pressure outlet	Pressure outlet	Pressure outlet
Turbulence Inlet	5 %	k & ε	30 %
Temperature	293 K	293 K	293 K
Reynolds Number	40,000	40,000	40,000
Grid elements	1.13e6	7.25e5	7.25e5

The boundary conditions for the full domain are a mass flow inlet and a pressure outlet with a gauge pressure of 0 Pa. The near-wall flow is modeled using the *enhanced wall treatment* by Fluent, which is capable of low-Reynolds-Number meshes as well as wall-function meshes [24]. Since the turbulence intensity is not exactly known in the test rig, 5 % are assumed as inflow condition. The influence of the degree of turbulence at the inlet of the plenum on the flow inside the mixing tube and the combustion chamber is expected to be relatively low, due to the flow acceleration in the orifice and the swirler passages.

For the LES a spectral synthesizer was used in order to imprint turbulence on the inlet flow. This was necessary since the axial jet tended to attach onto the wall of the mixing tube, when steady boundary conditions were applied. Such a behavior was neither observed in the experiment nor in the RANS simulations. Hence the given inflow velocity vectors are perturbed. A similar approach was investigated by Iudiciani and Duwig [23] for the simulation of a swirl-stabilized combustor, where the swirl generator was not included in the domain. In the referenced study a monochromatic excitation was impressed, whereas the present study uses a synthesizer which computes a divergence-free velocity fluctuation vector field from the summation of Fourier harmonics [25]. The fluctuation is scaled to match realistic turbulent length and time scales.

These scales are calculated from the degree of turbulence and a characteristic length, which are estimated by the experimental results and the geometry. In order to validate this approach for the current configuration, the velocity and turbulence profiles in the mixing tube and the combustion chamber are compared for the cases shown in Table 1. Prior to that, the sensitivity of the RANS simulations is assessed in terms of the spatial grid resolution. Therefore, the baseline mesh is refined in the area of interest leading to 2.12 million cells for the full mesh and to 1.57 million for the truncated case.

Both domains are meshed equally on the intersecting parts and in the reduced domain the same mesh is used for RANS and LES. The inner flow region consists of an unstructured tetrahedral mesh, while the boundary layers are refined by prism layers. Considering the turbulent length scales, the cell size is set to 0.5 mm in the mixing tube and 0.25 mm at the fuel injection. The mesh is refined in regions, where high velocity gradients are expected and coarsened towards the end of the combustion chamber.

The fuel injection holes are defined as a separated inlet boundary condition, which is independent from the main flow. Thus the amount of fuel injection can be directly varied. Fuel and water are both represented by isothermal water but modeled as a homogenous multicomponent configuration. Thus, the mixing quality can be calculated from the volume fraction of the fuel phase. In order to determine the volume fraction, the mixture model from Fluent is used, which is a simplified Eulerian multiphase model [24].

The LES was conducted with a constant time step in order to keep the courant number below $Co = 0.8$ to guarantee numerical stability. The results were time averaged after reaching a statistically steady state.

Experimental setup

The experiments were conducted in a vertical water tunnel as described in [26] where optical access was provided to the mixing tube and the combustion chamber. The Reynolds number resulted in $Re = 40{,}000$ with respect to the diameter of the mixing tube D, agreeing the simulations. Instantaneous 2D velocity fields of axial planes are obtained by using the non-intrusive optical Particle Image Velocimetry (PIV) method. The seeded (silver coated hollow glass spheres, 15 µm) water is illuminated by a double pulse Nd:YLF laser with a wavelength of 527 nm. A high speed CMOS-Camera was used to detect the scattered light. Cross-correlations and averaging over 1000 image pairs deliver the mean velocity field, which then is normalized with the mean bulk velocity u_0 at the burner exit. More detailed information concerning the experimental setup is given in [3].

In addition to the PIV measurements, the Planar Laser-Induced Fluorescence (PLIF) method is applied to crosswise planes, giving the quality of mixing between the main and the fuel flow. The fuel flow is supplied by an extra pump from a separated water tank and enriched with Rhodamine 6G dye. The tunnel is operated in open loop, whereas the PIV measurements are conducted in closed-loop. The amount of fuel injection remains the same as for the PIV measurements and for the simulations, where pure water is used as fuel simulant. The Rhodamine dye emits light of a wave length of 480 nm when excited by the laser. A band-pass filtered high-speed CMOS camera is sampling the light emissions with 1000 fps and 4 px/mm. The experimental setup for both methods is shown in Figure 3. For more details refer [6].

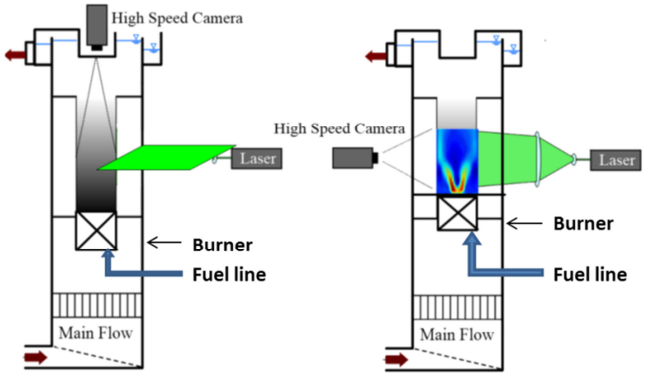

FIGURE 3: EXPERIMENTAL SETUP FOR MIXING EVALUATION AND PIV

Using background subtraction and the light intensity of a homogeneous concentration, the local concentration of the fuel simulant $C(x,t)$ is obtained from the intensity of the light emitted by the excited Rhodamine molecules $I(x,t)$:

$$C(x,t) = C_{\text{hom}} * \frac{I(x,t) - I_{back}(x,t)}{I_{\text{hom}}(x,t) - I_{back}(x,t)} \qquad \textbf{(13)}$$

The mixing quality is quantified by the Danckwerts unmixedness parameter U [27], which is defined as

$$U = \frac{\langle \left(\overline{C(x)} - \langle \bar{C} \rangle\right)^2 \rangle}{C_\infty * (1 - C_\infty)} \qquad \textbf{(14)}$$

Besides this scalar parameter a spatial distribution of the normalized concentration is used to show how the fuel agent distributes across the burner exit plane:

$$C^* = \overline{C(x)} / \langle \bar{C} \rangle \qquad \textbf{(15)}$$

RESULTS AND DISCUSSION

The current results are divided in three parts. First, a parameter study is conducted to examine the influence of the amount of axial injection onto the recirculation zone. Second, the validation of the flow field is presented by comparing the simulations of a single configuration to experimental PIV data obtained in the water tunnel. In the third part, the transient simulations are analyzed concerning periodic structures and the mixing quality of the air and fuel simulants.

To compare the cases, velocity profiles as well as the stagnation line of the axial velocity are used. Figure 4 shows the profile positions, from which two are located along the mixing tube and two in the combustion chamber. The most downstream profile cuts through the recirculation zone. Measuring a profile directly at the exit of the mixing tube was not possible due to limitations of the optical access in the experiments.

All geometric positions are normalized by the hydraulic diameter of the mixing tube. The x-axis is pointing in axial direction and its origin is located at the exit of the mixing tube. The velocity data is read out from an axial cross-section und normalized by the bulk velocity in the mixing tube.

Parameter study

A flow field that is suitable for a stable and fuel flexible combustion has to ensure that vortex breakdown establishes downstream of the burner exit, so the flame is not able to propagate upstream in the mixing tube. Moreover the recirculation should be not too far downstream in the combustion chamber. In order to identify the optimum amount of axial injection, a parameter study is conducted. Table 2 contains the choice of parameters. In a first study the orifice for the axial jet was changed from 4 mm to 10 mm, resulting in a change of the axial volume flow ratio χ from 3.1 % to 17.1 %. These simulations were done with a fuel injection of 250 l/h to represent a realistic combustion case. The corresponding momentum ratio between fuel and main flow is $J = 3.1$. In a second study the influence of the fuel injection was investigated for the $\chi = 15\,\%$ case. The numerical setup corresponds to case 1 of Table 1 with slightly changing mesh sizes.

TABLE 2: PARAMETER SETTINGS

#	Orifice D_{or}	$\chi = \dot{V}_{ax}/(\dot{V}_{ax} + \dot{V}_{sw})$	Fuel injection	Numerical case
1	4.0 mm	3.1 %	250 l/h	Case 1
2	6.0 mm	7.3 %	250 l/h	Case 1
3	8.0 mm	12.7 %	250 l/h	Case 1
4	8.8 mm	15.0 %	250 l/h	Case 1, 2 & 3
5	10.0 mm	17.1 %	250 l/h	Case 1
6	8.8 mm	16.4 %	0 l/h	Case 1
7	8.8 mm	14 %	450 l/h	Case 1

Figure 5 (left) presents the outcome of the parameter study. In the case of a small amount of axial flow ($\chi < 10\,\%$) the recirculation zone establishes inside the mixing tube, which would allow the flame to propagate into the mixing tube in a reacting case. The isothermal and the reacting flow field are not identical and in general it cannot be stated that the characteristics of the isothermal flow field also apply to the reacting case, but Reichel et al. [6] verified a certain similarity for the flow field upstream the flame by comparing PIV data from the water tunnel and the combustion test rig. Assuming this similarity, the burner configurations without or with a low axial injection ratio are probably not suitable for safe and reliable operation. The desired position of the vortex breakdown, slightly downstream the exit of the mixing tube, is reached with a medium amount of axial flow in the range of 12 % to 15 %.

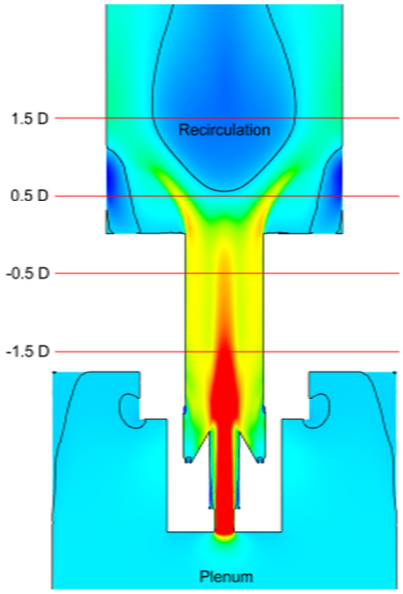

FIGURE 4: CONTOUR OF THE AXIAL VELOCITY OF THE FLOW FIELD INCLUDING THE ISOLINE OF AXIAL VELOCITY U=0 (BLACK) AND THE MEASUREMENT POSITIONS OF THE AXIAL VELOCITY AND TURBULENCE INTENSITY PROFILES (RED)

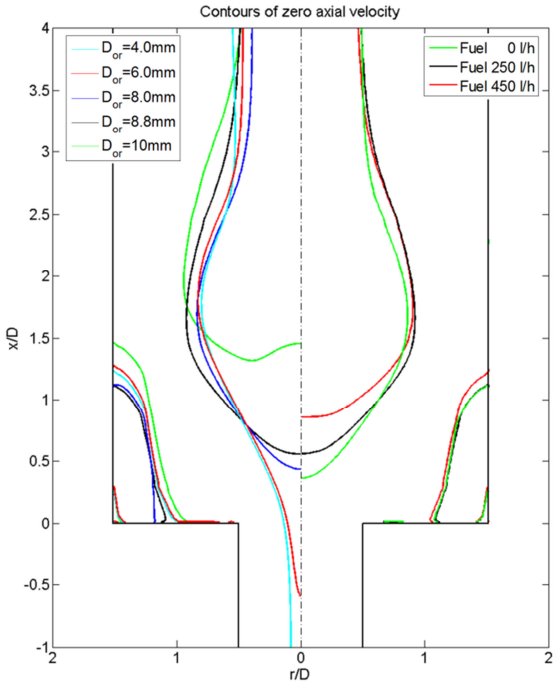

FIGURE 5: ISOLINES OF AXIAL VELOCITY U=0 FOR THE PARAMETER VARIATION OF THE ORIFICE DIAMETER WITH FUEL 250 L/H (LEFT) AND OF THE FUEL INJECTION WITH AN ORIFICE DIAMETER OF 8.8 MM (RIGHT)

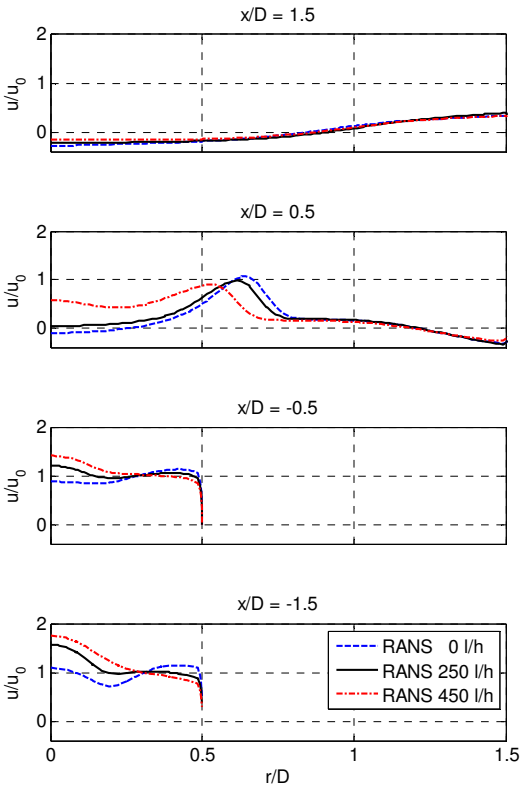

FIGURE 6: INFLUENCE OF AMOUNT OF FUEL INJECTION ON VELOCITY PROFILES (LEFT)

A further increase of the volume flow ratio leads to a downstream shift of the recirculation zone and, thus, of the flame position, which is not desirable to achieve a compact flame and high resistance against lean blow out. Consequently configuration #4 with $\chi = 15\,\%$ was chosen for the mixing investigation using LES and for the water tunnel based validation measurements.

The second parameter study shows that an increase of the fuel injection shifts the recirculation zone downstream (Figure 5 right) because of an enforced axial momentum. The fuel is injected coaxially, which means that the swirl intensity is reduced, resulting in higher axial velocities in the center line of the mixing tube and lower axial velocities near the wall (Figure 6). This effect is still present in the beginning of the combustion chamber, but at the most downstream location the profiles barely differ.

The amount of fuel injection also influences the axial volume flow ratio χ. As mentioned before, for a constant geometry the amount of axial flow depends only on the pressure conditions, since both inlets, the axial orifice and the swirler passages, are fed by the same plenum. The additional velocity of the fuel jets induces a low pressure region in the swirl passages, which forces more fluid to flow through the swirler. That explains the slightly decreasing χ for increased fuel injections. Nevertheless, the axial jet in the mixing tube is intensified by the rising fuel momentum.

Flow field validation

The simulations are validated for the configuration with $\chi = 15\,\%$ and a fuel injection rate of 250 l/h on the basis of the velocity and the turbulence intensity profiles located according to Figure 4. The turbulence intensity Tu is calculated in the following manners:

RANS: $$Tu = \frac{1}{u_0}\sqrt{\frac{2}{3}k} \quad \textbf{(16)}$$

LES: $$Tu = \frac{1}{u_o}\sqrt{\frac{1}{3}(u_{rms}^2 + v_{rms}^2 + w_{rms}^2)} \quad \textbf{(17)}$$

Experiments: $$Tu = \frac{1}{u_o}\sqrt{\frac{1}{3}(2u_{rms}^2 + v_{rms}^2)} \quad \textbf{(18)}$$

At first, the results of a mesh study are presented. This study is done with two different grid sizes in the full and the reduced (cropped) domain. As presented in Figure 8, the profiles of axial velocity collapse for all four configurations. The mesh study was conducted with RANS simulations due to the higher computational costs of LES. For both numerical domains, the full and the cropped one, the profiles of the axial velocity as well as of the turbulence intensity (Figure 9) are well in line with each other. Hence, for similar inflow conditions (same orifice and fuel injection), the cropped domain is assumed to be valid for reducing the mesh size. Since this behavior is also expected for the transient case, the usage of the cropped domain is able to reduce the computational effort significantly.

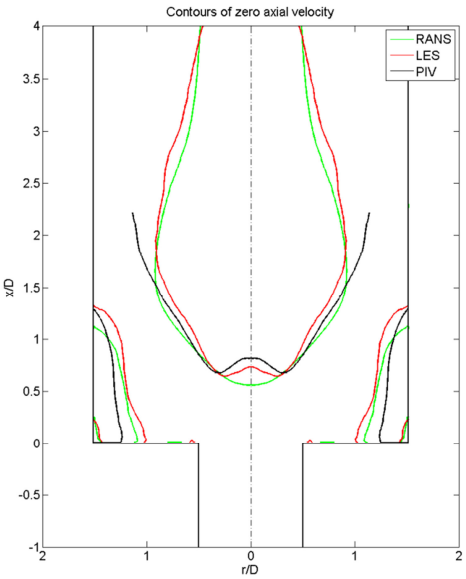

FIGURE 7: ISOLINES OF AXIAL VELOCITY U=0 FOR RANS, LES AND EXPERIMENT

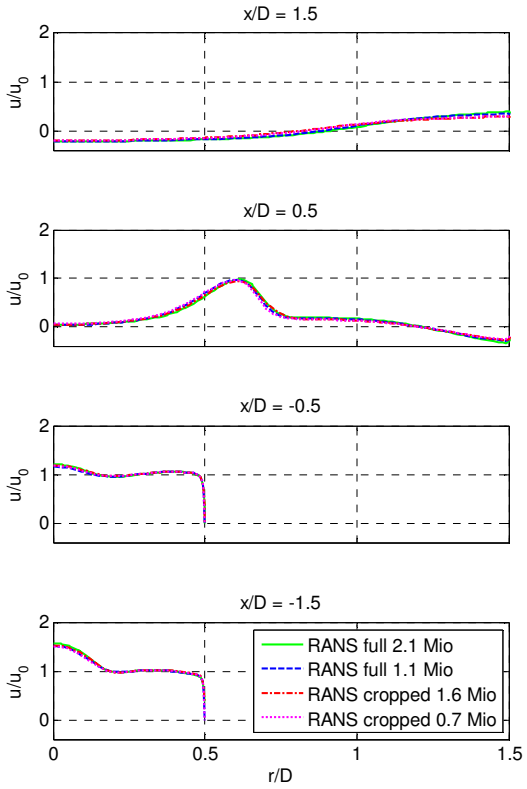

FIGURE 8: PROFILES OF AXIAL VELOCITY FOR TWO DIFFERENT GRID SIZES PER DOMAIN TYPE

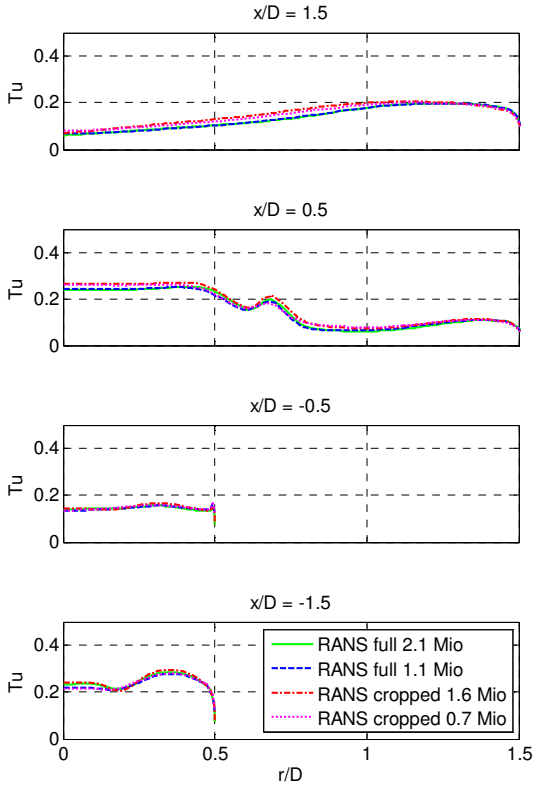

FIGURE 9: PROFILES OF THE TURBULENCE INTENSITY FOR TWO DIFFERENT GRID SIZES PER DOMAIN

Figure 10 shows profiles of the axial velocity resulting from RANS, LES and PIV. The velocity profiles of the RANS simulation and the measurement match well at all four positions. In general, the flow characteristic in the mixing tube is quite constant with a slightly decreasing axial jet at the center line. After passing the step diffusor into the combustion chamber, vortex breakdown establishes, characterized by a velocity deficit in the center (Figure 10) that results in a recirculation zone (Figure 7). The position of the vortex breakdown and the corresponding stagnation point play an important role for the flame stabilization. Therefore, the correct prediction of the recirculation zone's form is of special interest. Figure 7 shows that the isolines of simulation and experiment match well except for a small excess of the axial jet along the center line.

Using RANS the level of turbulence is well predicted at the most upstream position in the mixing tube and in the combustion chamber (Figure 11). In the downstream part of the mixing tube the turbulence intensity is under-predicted by the realizable k-ε turbulence model. The same underestimation was found for swirling flows by Schrödinger et al. [28].

While the outcome of the RANS simulation is a steady state flow field, the transient data from the LES has to be time-averaged for comparison. Regarding the profiles, the LES reveals a good agreement with the experimental velocity profiles inside the combustion chamber. The same applies for the location of the stagnation line and the turbulence intensity. Thus, it can be expected that the recirculation zone for the isothermal case will be well predicted by RANS as well as LES.

The velocity profiles inside the mixing tube also match the experimental profiles, but there is a deviation in the turbulence distribution at the most upstream position, where the degree of turbulence is under-predicted in the axial jet. Due to natural production and diffusion of turbulent kinetic energy, the turbulence intensity increases along the center line, but is still too low at the second measuring position. Further downstream, in the combustion chamber, the turbulence intensity of the LES matches well the experimental data. The turbulence at the beginning of the mixing tube strongly depends on the inflow boundary conditions, especially on the settings of the spectral synthesizer. The spectral synthesizer takes as input the length and time scales of the turbulence to generate an appropriate velocity fluctuation field that features the same scales. In the absence of experimental data from the swirler passages and the inlet of the axial jet, the scales where extrapolated from the mixing tube. According to the results, the degree of turbulence was slightly under-estimated at the inlet of the axial jet.

Setting up the synthesizer with k and ϵ from the RANS simulation (full domain) delivered no appropriate result, even though the degree of turbulence was well predicted by RANS in the most upstream position of the mixing tube (Figure 11).

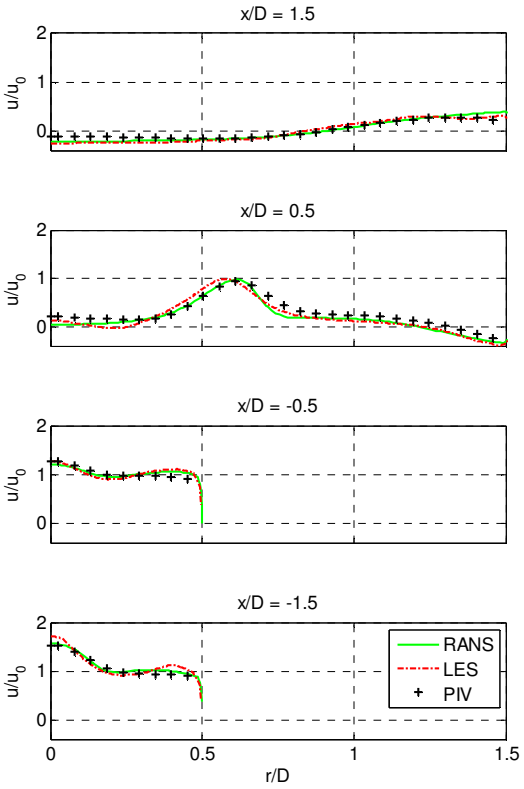

FIGURE 10: PROFILES OF AXIAL VELOCITY WITH 8.8 MM AXIAL ORIFICE AND 250 L/H FUEL INJECTION

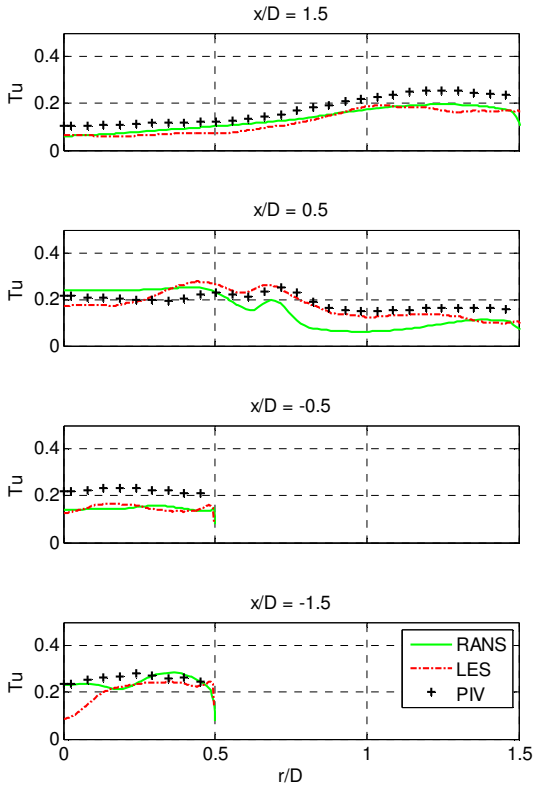

FIGURE 11: PROFILES OF TURBULENCE INTENSITY WITH 8.8 MM AXIAL ORIFICE AND 250L/H FUEL INJECTION

Of importance for the investigation of swirling flows are also the tangential velocities. A comparison between simulation and experiment is shown in Figure 12. Since the PIV measurements are not conducted as stereo PIV, the existing data of experimental tangential flow velocities is limited to the cases, where a flow field of a tangential plane was measured, which was only done for two axial positions and without appropriate fuel injection. Thus, this data can only be used for a validation of the RANS simulation. For both positions, one inside the mixing tube and one in the combustion chamber, the maximum tangential velocities are slightly over-estimated in the simulation. Comparing the steady and the transient simulation for the case with a fuel injection of 250 l/h, the RANS result is also delivering a higher peak. According to the RANS profiles, the influence of the fuel injection on the tangential velocity is low. Thus, it can be assumed, that the LES results match well to a realistic water tunnel flow.

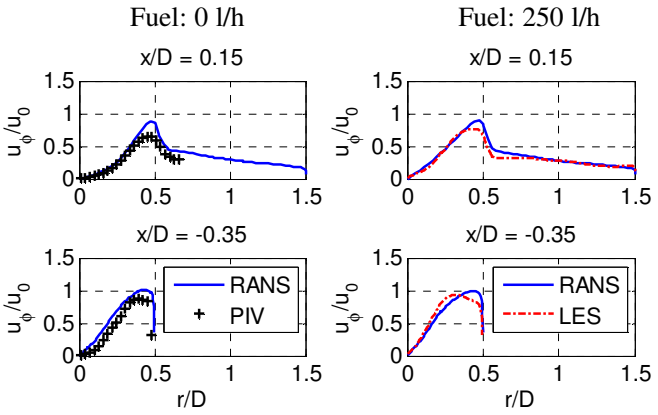

FIGURE 12: TANGENTIAL VELOCITY PROFILES FOR RANS AND PIV WITHOUT FUEL INJECTION (LEFT) AS WELL AS RANS AND LES WITH FUEL INJECTION (RIGHT)

Mixing investigation

Beside the velocity field, the fuel mixing is an important outcome of the isothermal simulation and will be discussed in the following part. To get an impression of the mixing process in the premixing section, a contour plot of the volume fraction of the fuel phase is given in Figure 13. There is no fuel in the inner part of the axial jet according to the RANS simulation. Most of the fuel is accumulated in a hollow cylinder (red) between the axial jet and the outer swirling flow. This behavior differs from experimental visualizations by Reichel et al. [6], which show that the fuel is equally distributed over the radius at the burner exit (except the near wall region) as depicted in Figure 14. The diffusion between the axial and the swirled flow as well as the turbulence intensity (Figure 11) seems to be under-predicted by the turbulence model.

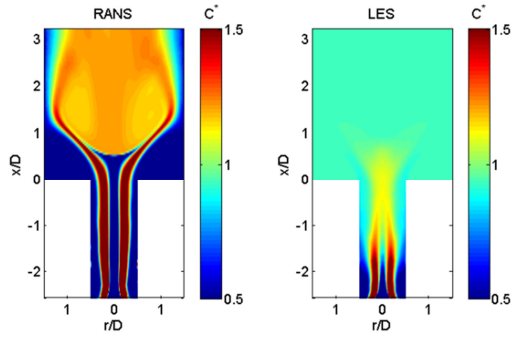

FIGURE 13: SPATIAL DISTRIBUTION OF TIME-AVERAGED, NORMALIZED CONCENTRATION OF THE FUEL AGENT FROM RANS (LEFT) AND LES (RIGHT) DATA

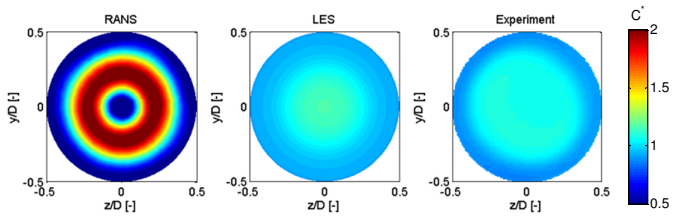

FIGURE 14: SPATIAL DISTRIBUTION OF TIME-AVERAGED, NORMALIZED CONCENTRATION OF THE FUEL AGENT AT THE BURNER EXIT IN THE RANS (LEFT), THE LES (CENTER) AND THE EXPERIMENT (RIGHT)

In the first part of the mixing tube the time-averaged fuel concentration of the LES is similar to the one of the RANS simulation (Figure 13). After this initial length the two fuel jets (in the planar representation) begin to merge due to turbulent mixing. At the burner exit the fuel agent is equally distributed in the area of the axial jet. As stated in the previous section, the turbulence intensity is slightly under-estimated in the mixing tube by the LES. Thus the turbulent diffusion is lower than in the experiment and the spatial distribution in the burner exit (Figure 14) plane shows a higher fuel concentration in the center of the mixing tube. This leads to a deviation in the spatial unmixedness U, which is negligibly small compared to the RANS results (Figure 15 left). Thus the LES delivers reasonable agreement to the experiment and a sufficient spatial mixing is ensured by the flow field even at high rates of axial injection.

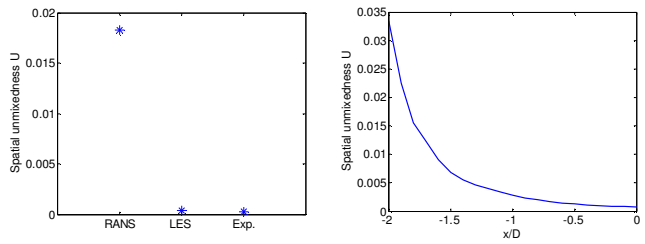

FIGURE 15: SPATIAL UNMIXEDNESS AT THE BURNER EXIT IN THE RANS, THE LES AND THE EXPERIMENT (LEFT) AND ALONG THE MIXING TUBE CALCULATED FROM LES RESULTS (RIGHT)

The contour of the volume fraction (Figure 13) already shows how the mixing develops over the length of the mixing tube. In Figure 15 (right) this development is quantified using the spatial unmixedness. The unmixedness is decreasing strongly in the beginning of the mixing tube and reaches saturation towards the end. It can be concluded that an extension of the mixing tube will not further improve the mixing quality significantly.

Flow dynamics

The LES delivers transient data, which is sampled at a frequency of 2000 Hz for the whole velocity and volume fraction field. Figure 16, showing a time-averaged RMS contour of the axial velocity at a longitudinal cross-section, indicates that the highest fluctuations of the axial velocity can be expected near the burner exit and along the shear layers of the recirculation zone. In order to assess the unsteady behavior of the flow field, a spectrum of the turbulent kinetic energy was computed from the points A, B and C, located in the middle cross-section and presented in Figure 16 (left). Point A lies in the shear layer, point B in the central axis where the non-swirling axial jet enters the combustion chamber and point C in the mixing tube upstream of the area expansion. The same points are depicted in Figure 16 (right), showing the instantaneous behavior of the flow by an arbitrary snapshot of the axial velocity in the central plane of the combustor.

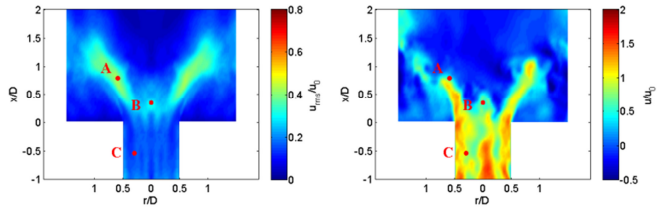

FIGURE 16: TIME-AVERAGED RMS CONTOUR (LEFT) AND INSTANTANEOUS SNAPSHOT (RIGHT) OF THE AXIAL VELOCITY AT THE BURNER EXIT WITH THE POINTS THAT ARE USED FOR THE SPECTRAL ANALYSIS

The energy spectrum describes the energy cascade from large-scale vortices to small-scale turbulence. In Figure 17 the energy is drawn over a normalized frequency, called the Strouhal number:

$$St = \frac{fD}{u_0} \tag{19}$$

On the one hand, the energy spectrum delivers a validation for the simulation itself. The spectral turbulent kinetic energy is plotted against the -5/3 power law by Kolmogorov, which describes the energy transition in the inertial subrange. Since the simulation result matches well this slope, it can be concluded that the mesh is fine enough for predicting the turbulence reasonably.

On the other hand, the spectrum yields a closer look in the unsteady behavior since it is capable of identifying periodicities in the flow field. For a similar configuration García-Villalba et

al. [29] stated that coherent structures, like a precessing vortex core, are related to a dominant frequency. For none of the mentioned positions a clear peak can be observed from the turbulent energy spectra. Reichel et al. [6] showed for the same combustor, but without the non-swirling jet, that a hydrodynamic instability clearly manifests in the energy spectrum, which then was suppressed by the axial jet (Figure 18). However, it cannot be guaranteed that there is no oscillation at all. In fact, experimental studies on a very similar combustor revealed a very weak coherent structure located comparably far downstream in the combustor ([9]). Nevertheless the results imply that there is at least no strong coherent structure in the flow field of the combustion chamber.

The comparison of the spectra in the combustion chamber to the one in the mixing tube (C) shows that the energy is shifted to higher frequencies in the mixing passage.

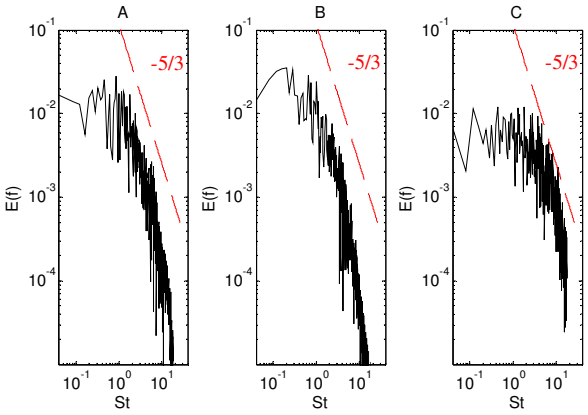

FIGURE 17: TURBULENT KINETIC ENERGY SPECTRA DETERMINED FOR A POINT IN THE SHEAR LAYER (A), A POINT AT THE CENTRAL AXIS (B) AND A POINT IN THE MIXING TUBE (C) TOGETHER WITH A -5/3 SLOPE

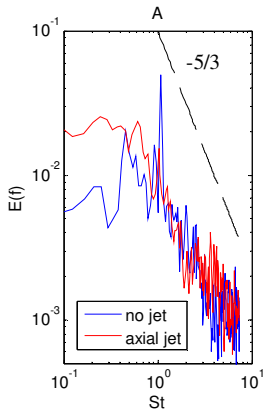

FIGURE 18: TURBULENT KINETIC ENERGY SPECTRUM AT POINT A FROM PIV DATA WITH (RED) AND WITHOUT (BLUE) AXIAL INJECTION

Despite the swirl, the flow field seems to be unaffected by large scale hydrodynamic instabilities. The aforementioned thesis by various authors ([7, 10, 11, 16]), stating that the presence of a non-swirling axial jet is able to suppress the presence of large scale coherent structures, can be confirmed for the investigated configuration.

CONCLUSIONS

The present paper presents numerical simulations of an isothermal flow in a swirl-stabilized burner. The aim of this study is the investigation of the mixing process in a swirl burner with a non-swirling axial jet. For the turbulence modeling both the Reynolds Averaged Navier-Stokes simulations as well as Large Eddy Simulation were employed. The results were compared to experimental data obtained with PIV in a water tunnel.

In a first step a parameter study was conducted using RANS simulations. Therefore, the mass flow ratio between the axial jet and the flow through the swirler passage was varied by geometry modifications. The optimal amount of axial air to establish a stable vortex breakdown downstream the burner exit was found for $\chi = 15\ \%$. The validation of this case in the water tunnel showed an excellent agreement for RANS as well as LES regarding the velocity field in the mixing tube and the combustion chamber. Utilizing the realizable k-ε turbulence model, the steady-state simulations were not capable of giving a realistic mixing of the fuel and the main flow.

This task is sufficiently fulfilled by the LES. The spatial unmixedness is in good agreement with the measurements. Furthermore the spectral analysis of the transient data concludes that the flow field is quite stable along the combustion zone. The turbulent energy spectra do not reveal a dominant frequency implying that no strong coherent structure is present.

ACKNOWLEDGEMENT

The presented paper is part of the work performed in the context of the project CLEAN GT supported by Climate KIC, the EU's main climate innovation initiative. The experimental data was gained in research that has received funding from the European Union Seventh Framework Program (FP7/2007-2013) under grant agreement n° 284636 and the European Research Council under the ERC grant agreement n° 247322, GREENEST.

REFERENCES

[1] A. H. Lefebvre and D. R. Ballal, *Gas turbine combustion: Alternative fuels and emissions*, 3rd ed. Boca Raton: Taylor & Francis, 2010.

[2] K. Döbbeling and J. Hellat, "25 Years of BBC/ABB/Alstom Lean Premix Combustion Technologies," *Journal of Engineering for Gas Turbines and Power*, vol. 129, no. 1, 2007.

[3] T. Reichel, S. Terhaar, and C. O. Paschereit, "Increasing Flashback Resistance in Lean Premixed Swirl-Stabilized Hydrogen Combustion by Axial Air Injection," *Journal of Engineering for Gas Turbines and Power*, Nov. 2014.

[4] S. Burmberger and T. Sattelmayer, “Optimization of the Aerodynamic Flame Stabilization for Fuel Flexible Gas Turbine Premix Burners,” *Journal of Engineering for Gas Turbines and Power*, vol. 133, no. 10, 2011.

[5] S. Burmberger, C. Hirsch, and T. Sattelmayer, “Designing a Radial Swirler Vortex Breakdown Burner,” in *Volume 1: Combustion and Fuels, Education*, 2006, vol. 2006, pp. 423–431.

[6] T. G. Reichel, S. Terhaar, and C. O. Paschereit, “Flow Field Manipulation by Axial Air Injection to Achieve Flashback Resistance and its Impact on Mixing Quality,” *43rd Fluid Dynamics Conference*, Jun. 2013.

[7] O. Lucca-Negro and T. O’Doherty, “Vortex breakdown: a review,” *Progress in Energy and Combustion Science*, vol. 27, no. 4, pp. 431–481, Jan. 2001.

[8] Y. Huang and V. Yang, “Dynamics and stability of lean-premixed swirl-stabilized combustion,” *Progress in Energy and Combustion Science*, vol. 35, no. 4, pp. 293–364, Aug. 2009.

[9] S. Terhaar, T. G. Reichel, C. Schrödinger, L. Rukes, C. O. Paschereit, and K. Oberleithner, “Vortex Breakdown Types and Global Modes in Swirling Combustor Flows with Axial Injection,” *Journal of Propulsion and Power*, pp. 1–11, May 2014.

[10] S. Terhaar, O. Krüger, and C. O. Paschereit, “Flow Field and Flame Dynamics of Swirling Methane and Hydrogen Flames at Dry and Steam-Diluted Conditions,” *Proceedings of the ASME Turbo Expo 2014*, Jun. 2014.

[11] P. Jochmann, A. Sinigersky, R. Koch, and H.-J. Bauer, “URANS Prediction of Flow Instabilities of a Novel Atomizer Combustor Configuration,” *ASME Turbo Expo 2005*, pp. 19–27, 2005.

[12] A. Spencer, J. J. McGuirk, and K. Midgley, “Vortex Breakdown in Swirling Fuel Injector Flows,” *Journal of Engineering for Gas Turbines and Power*, vol. 130, no. 2, p. 021503, 2008.

[13] K. Midgley, A. Spencer, and J. J. McGuirk, “Unsteady Flow Structures in Radial Swirler Fed Fuel Injectors,” *Journal of Engineering for Gas Turbines and Power*, vol. 127, no. 4, p. 755, 2005.

[14] M. García-Villalba, J. Fröhlich, and W. Rodi, “Numerical Simulations of Isothermal Flow in a Swirl Burner,” *Journal of Engineering for Gas Turbines and Power*, vol. 129, no. 2, p. 377, 2007.

[15] C. Duwig and L. Fuchs, “Large eddy simulation of vortex breakdown/flame interaction,” *Physics of Fluids*, vol. 19, no. 7, p. 075103, 2007.

[16] R. Spall and T. Gatski, “Numerical calculations of three-dimensional turbulent vortex breakdown,” *International Journal for Numerical Methods in Fluids*, vol. 20, pp. 307–318, 1995.

[17] J. Z. T.-H. Shih, W.W. Liou, A. Shabbir, Z. Yang, “A New k-ε Eddy-Viscosity Model for High Reynolds Number Turbulent Flows - Model Development and Validation,” *Computers Fluids*, vol. 24(3), pp. 227–238, 1995.

[18] J. O. Hinze, *Turbulence*. New York: McGraw-Hill Publishing Co, 1975.

[19] J. Smagorinsky, “General Circulation Experiments with the Primitive Equations. I. The Basic Experiment,” *Month.Wea. Rev.*, vol. 91, pp. 99–164, 1963.

[20] O. Krüger, C. Duwig, S. Terhaar, and C. O. Paschereit, “Numerical Investigations and Modal Analysis of the Coherent Structures in a Generic Swirl Burner,” in *21st AIAA Computational Fluid Dynamics Conference*, 2013.

[21] J. L. XIA, B. L. Smith, A. C. Benim, J. Schmidli, and G. Yadigaroglu, “Effect of Inlet and Outlet Boundary Conditions on Swirling Flows,” *Computers & Fluids*, vol. 26, no. 8, pp. 811–823, 1997.

[22] A. C. Benim, M. P. Escudier, A. Nahavandi, K. Nickson, and K. J. Syed, “DES Analysis of Confined Turbulent Swirling Flows in the Sub-critical Regime,” pp. 172–181, 2008.

[23] P. Iudiciani and C. Duwig, “Large Eddy Simulation of the Sensitivity of Vortex Breakdown and Flame Stabilisation to Axial Forcing,” *Flow, Turbulence and Combustion*, vol. 86, no. 3–4, pp. 639–666, Feb. 2011.

[24] I. Ansys, *ANSYS FLUENT Theory Guide, ANSYS FLUENT Release 14.5*. Southpointe: ANSYS, Inc., 2012.

[25] A. Smirnov, S. Shi, and I. Celik, “Random Flow Generation Technique for Large Eddy Simulations and Particle-Dynamics Modeling,” *Journal of Fluids Engineering*, vol. 123, pp. 359–371, 2001.

[26] A. Lacarelle and C. O. Paschereit, “Increasing the Passive Scalar Mixing Quality of Jets in Crossflow With Fluidics Actuators,” *Journal of Engineering for Gas Turbines and Power*, vol. 134, no. 2, p. 021503, 2012.

[27] P. V. Danckwerts, “The definition and measurement of some characteristics of mixtures,” *Applied Scientific Research*, vol. 3, no. 4, pp. 279–296, 1952.

[28] C. Schrödinger, O. Krüger, A. Lacarelle, M. Oevermann, and C. O. Paschereit, “CFD Modeling of the Influence of Fuel Staging on the Mixing Quality and Flame Characteristics in a Lean Premixed Combustor,” *Proceedings of ASME Turbo Expo 2010*, 2010.

[29] M. García-Villalba, J. Fröhlich, and W. Rodi, “Identification and analysis of coherent structures in the near field of a turbulent unconfined annular swirling jet using large eddy simulation,” *Physics of Fluids*, vol. 18, no. 5, p. 055103, 2006.